Unsupervised Change Detection in Satellite Images Using Principal Component Analysis and k-Means Clustering

Turgay Celik

***Abstract*—In this letter, we propose a novel technique for unsupervised change detection in multitemporal satellite images using principal component analysis (PCA) and k-means clustering. The *difference image* is partitioned into $h \times h$ nonoverlapping blocks. S, $S \leq h^2$, orthonormal eigenvectors are extracted through PCA of $h \times h$ nonoverlapping block set to create an eigenvector space. Each pixel in the *difference image* is represented with an S-dimensional feature vector which is the projection of $h \times h$ *difference image* data onto the generated eigenvector space. The change detection is achieved by partitioning the feature vector space into two clusters using k-means clustering with $k = 2$ and then assigning each pixel to the one of the two clusters by using the minimum Euclidean distance between the pixel's feature vector and mean feature vector of clusters. Experimental results confirm the effectiveness of the proposed approach.**

***Index Terms*—Change detection, k-means clustering, multitemporal satellite images, optical images, principal component analysis (PCA), remote sensing.**

I. Introduction

CHANGE detection methods could be categorized as either supervised or unsupervised according to the nature of data processing. The former is based on a supervised classification method, which requires the availability of a ground truth in order to derive a suitable training set for the learning process of classifiers. The latter approach, which is adopted in this letter, performs change detection by making a direct comparison of two multitemporal images considered without incorporating any additional information.

Unsupervised change detection techniques mainly use the automatic analysis of change data which are constructed using multitemporal images. The change data are generally created using one of the following: 1) *image differencing*; 2) *normalized difference vegetation index*; 3) *change vector analysis*; 4) *principal component analysis (PCA)*; and 5) *image rationing* [1]. Several unsupervised change detection techniques have been proposed in the literature falling in these categories [2]–[4] which use complicated data modeling and parameter estimation.

Most of the unsupervised methods are developed based on the image differencing. Image differencing-based algorithms accomplish the change detection by subtracting, on a pixel basis, the images acquired at two time instances to produce new image called *difference image*. The computed difference image is such that the values of the pixels associated with land cover or land use changes present values significantly different from those of the pixels associated with unchanged areas. Changes are then identified by analyzing the difference image. In [5], two automatic techniques based on the Bayes theory for the analysis of the difference image are proposed. One allows an automatic selection of the decision threshold for maximizing the overall change detection error under the assumption that the pixels of difference image are spatially independent (expectation-maximization (EM)-based thresholding). The other analyzes the difference image by considering the spatial contextual information included in the neighborhood of each pixel. This approach based on the Markov random fields (MRFs) exploits the context of interpixel class dependence (MRF-based thresholding). The algorithm requires high computational power and is not feasible to be applied for near-real-time change detection purposes. There are many other change detection methods using the same framework for synthetic aperture radar (SAR) images [6], [7] and achieved satisfactory results by using complicated data modeling and parameter estimation. However, these methods are applied to the raw data domain and suffer from the inference of speckle noise.

In this letter, a computationally simple yet effective automatic change detection method is proposed by analyzing the difference image of two satellite images acquired from the same area coverage but at two different time instances. The nonoverlapping blocks of the difference image are used to extract eigenvectors by applying PCA [8]. Then, a feature vector for each pixel of the difference image is extracted by projecting its $h \times h$ neighborhood data onto eigenvector space. The feature vector space is clustered into two clusters using k-means algorithm [8]. Each cluster is represented with a mean feature vector. Finally, change detection is achieved by assigning each pixel of the difference image to the one of the clusters according to the minimum Euclidean distance between its feature vector and mean feature vector of the clusters.

This letter is organized as follows. Section II describes the proposed unsupervised change detection approach. Section III provides some experimental results of the proposed approach for both noise-free and noisy images and comparisons with the state-of-the-art methods proposed in [5]. Section IV concludes this letter.

Manuscript received March 25, 2009; revised April 22, 2009. First published August 7, 2009; current version published October 14, 2009. This work was supported by the Singapore Ministry of Education under Grant R-143-000-358-112.

The author is with the Department of Chemistry, Faculty of Science, National University of Singapore, Singapore 117543 (e-mail: chmcelik@nus.edu.sg; celikturgay@gmail.com).

Digital Object Identifier 10.1109/LGRS.2009.2025059

1545-598X/$26.00 © 2009 IEEE

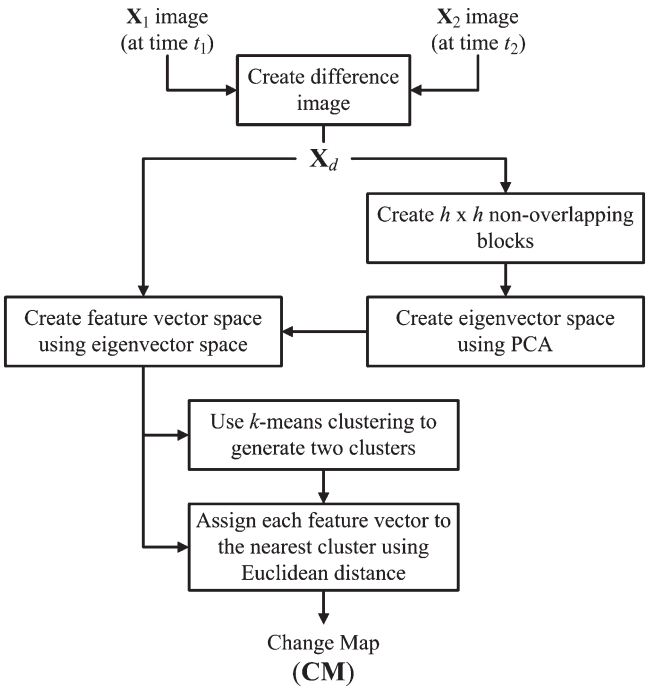

Fig. 1. General scheme of the proposed approach.

II. Proposed Change Detection Technique

Let us consider two coregistered satellite intensity images, $\mathbf{X}_1 = \{x_1(i,j)|1 \le i \le H, 1 \le j \le W\}$ and $\mathbf{X}_2 = \{x_2(i,j)|1 \le i \le H, 1 \le j \le W\}$, with a size of $H \times W$, each acquired at the same geographical area but at two different time instances, t_1 and t_2, respectively. We aim at generating a change detection map, so-called *change map*, that represents changes that occurred on the ground between the acquisition dates of the two images $\mathbf{X}_1$ and $\mathbf{X}_2$. The change detection problem can be modeled as a binary classification problem. Let $\Omega = \{w_c, w_u\}$ be the set of classes associated with *changed* (denoted by w_c) and *unchanged* (denoted by w_u) pixels on the images $\mathbf{X}_1$ and $\mathbf{X}_2$. The proposed approach is made up of the following six main steps (see Fig. 1): 1) generation of the difference image; 2) generation of $h \times h$ nonoverlapping image blocks from the difference image; 3) creating eigenvector space using PCA on $h \times h$ nonoverlapping image blocks; 4) creating a feature vector space over the entire difference image by projecting overlapping $h \times h$ data blocks around each pixel onto eigenvector space; 5) clustering feature vector space into two clusters corresponding to w_u and w_c using k-means algorithm with $k = 2$; and 6) generation of the change map by assigning each pixel of the difference image to the one of the clusters according to the minimum Euclidean distance between its feature vector and the mean feature vector of the clusters.

The first step of the proposed algorithm is generating the difference image. Let $\mathbf{X}_d$ be the difference image, and it can be defined differently with respect to the type of input image. For the optical images, $\mathbf{X}_d$ can be defined as absolute-valued difference of intensity values of two images, i.e.,

$$\mathbf{X}_d = |\mathbf{X}_2 - \mathbf{X}_1|. \tag{1}$$

The second step of the proposed approach is partitioning $\mathbf{X}_d$ into $h \times h$ nonoverlapping blocks, where $h \ge 2$. Let $\mathbf{X}_d(y,x) = \{x_d(m,n)|y - \lceil h/2 \rceil + 1 \le m \le y + h - \lceil h/2 \rceil, x - \lceil h/2 \rceil + 1 \le n \le x + h - \lceil h/2 \rceil\}$ be $h \times h$ difference-image block referenced by (centered at when h is odd) coordinates (y,x), where $\lceil\ \rceil$ is a mathematical ceiling operator which rounds a number up, to the nearest integer, e.g., $\lceil 2.5 \rceil = 3$. Using the lexicographically ordering of $\mathbf{X}_d(y,x)$, the vector formulation can be obtained

$$\mathbf{x}_d(y,x) = \begin{bmatrix} x_d\left(y - \lceil h/2 \rceil + 1, x - \lceil h/2 \rceil + 1\right) \\ \vdots \\ x_d\left(y - \lceil h/2 \rceil + 1, x\right) \\ \vdots \\ x_d\left(y - \lceil h/2 \rceil + 1, x + h - \lceil h/2 \rceil\right) \\ \vdots \\ x_d(y,x) \\ \vdots \\ x_d\left(y + h - \lceil h/2 \rceil, x - \lceil h/2 \rceil + 1\right) \\ \vdots \\ x_d\left(y + h - \lceil h/2 \rceil, x\right) \\ \vdots \\ x_d\left(y + h - \lceil h/2 \rceil, x + h - \lceil h/2 \rceil\right) \end{bmatrix}. \tag{2}$$

The set of vectors $\mathbf{x}_d(y,x)$ is used to create an eigenvector space using PCA [8]. For ease of mathematical notation, $\mathbf{x}_d^p$ is used to denote the vector $\mathbf{x}_d(y,x)$, while p represents an index with $1 \le p \le M = \lfloor (H \times W)/(h \times h) \rfloor$, where $\lfloor\ \rfloor$ is a mathematical floor operator which rounds a number down, to the nearest integer. The average vector of the set is defined by

$$\mathbf{\Psi} = \frac{1}{M} \sum_{p=1}^{M} \mathbf{x}_d^p. \tag{3}$$

Each vector differs from the average vector by the vector $\mathbf{\Delta}_p = \mathbf{x}_d^p - \mathbf{\Psi}$. The PCA, which seeks a set of N orthonormal vectors $\mathbf{e}_s$ and their associated scalars λ_s which best describe the distribution of the data, is applied on the difference vector set $\mathbf{\Delta}_p$. The vectors $\mathbf{e}_s$ and corresponding scalars λ_s are the eigenvectors and eigenvalues, respectively, of the covariance matrix

$$\mathbf{C} = \frac{1}{M} \sum_{p=1}^{M} \mathbf{\Delta}_p \mathbf{\Delta}_p^{\mathrm{T}} \tag{4}$$

where $()^T$ corresponds to transpose of the vector. The matrix $\mathbf{C}$ is $h^2 \times h^2$ and determines h^2 eigenvectors and eigenvalues. Let us assume that the generated eigenvectors of $\mathbf{C}$ are sorted in descending order with respect to their eigenvalues, i.e., $\lambda_s \ge \lambda_{s+1}$.

The feature vector space is created by projecting $\mathbf{x}_d(i,j)$ onto eigenvector space for each pixel at spatial location (i,j), i.e.,

$$\mathbf{v}(i,j) = \begin{bmatrix} v_1 & v_2 & \cdots & v_S \end{bmatrix}^{\mathrm{T}} \tag{5}$$

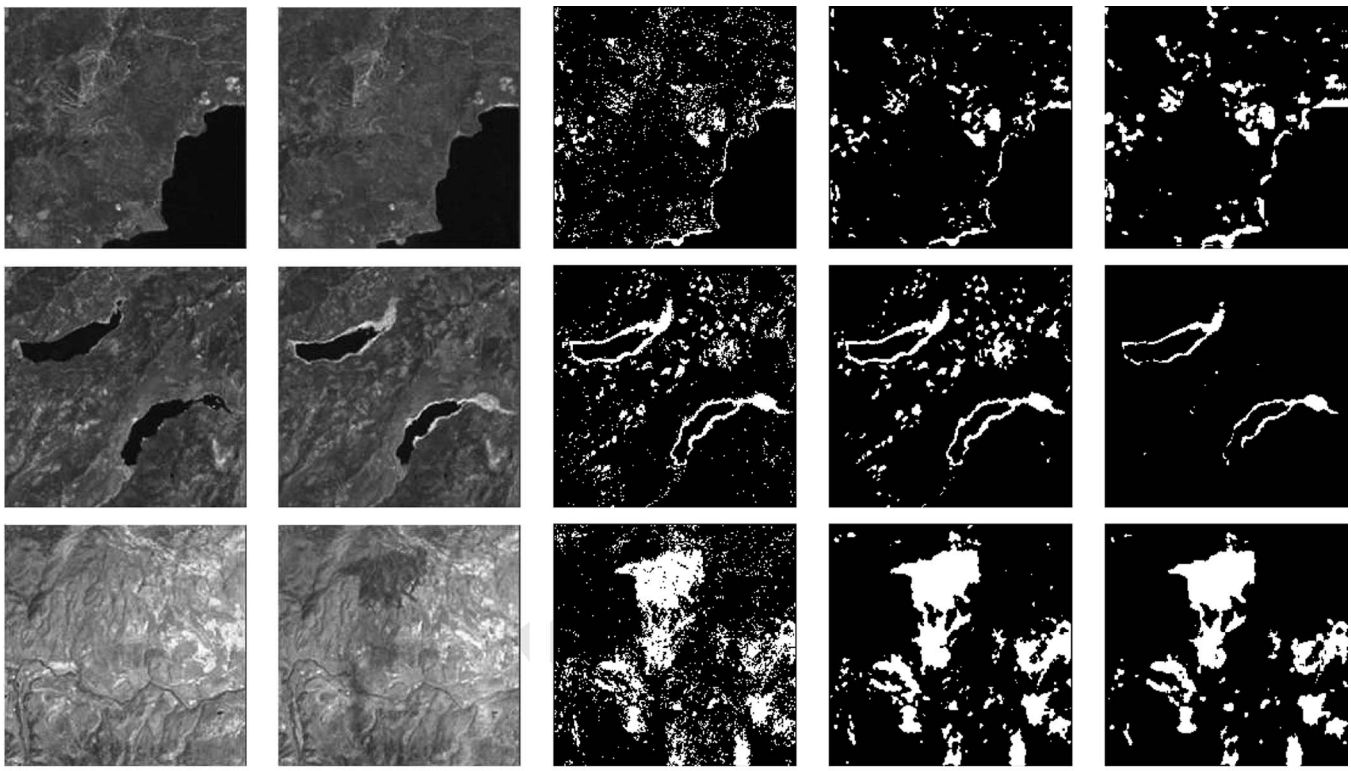

Fig. 2. Change detection results for different approaches on optical images. (a) Input image $\mathbf{X}_1$. (b) Input image $\mathbf{X}_2$. (c) EM-based thresholding [5]. (d) MRF-based thresholding when $\beta = 1.6$ [5]. (e) Proposed approach.

where $1 \leq S \leq h^2$ and $v_s = \mathbf{e}_s^{\mathrm{T}}(\mathbf{x}_d(i,j) - \mathbf{\Psi})$, $1 \leq s \leq S$. The parameter S determines the dimension of the feature vector $\mathbf{v}(i,j)$ at spatial location (i,j) and is simply the number of eigenvectors used in projecting $\mathbf{x}_d(i,j)$ onto eigenvector space. The vector $\mathbf{x}_d(i,j)$ is obtained the same way with (2).

The next stage of the proposed approach is the generation of two clusters by clustering the feature vector space using the k-means clustering algorithm, where $k = 2$. Let $\mathbf{v}_{w_u}$ and $\mathbf{v}_{w_c}$ be cluster mean feature vector for classes w_u and w_c, respectively. In order to label clusters generated by the k-means clustering algorithm with the labels w_u and w_c, the labeled pixels from k-means clustering algorithm are used to find two average values over the difference image. When there is a change between two images in a specific region, then it is expected that the values of the difference image pixels in that region are higher than the values of pixels in the regions where there is no change. Using this assumption, the cluster whose pixels have lower average value in the difference image is assigned as the w_u class, and the other cluster is assigned as w_c class.

Using $\mathbf{v}_{w_c}$ and $\mathbf{v}_{w_u}$, a binary change map $\mathbf{CM} = \{\mathrm{cm}(i,j) | 1 \leq i \leq H, 1 \leq j \leq W\}$ can be created, in which "1" indicates that the corresponding pixel location involves a change (i.e., belonging to w_c class), whereas "0" involving no changes (i.e., belonging to w_u class). This process can be viewed as *unsupervised thresholding* according to

$$\mathrm{cm}(i,j) = \begin{cases} 1, & \|\mathbf{v}(i,j) - \mathbf{v}_{w_c}\|_2 \leq \|\mathbf{v}(i,j) - \mathbf{v}_{w_u}\|_2 \\ 0, & \text{otherwise} \end{cases} \tag{6}$$

where $\| \ \|_2$ is Euclidean distance.

III. Experimental Results

In order to assess the effectiveness of the proposed approach, we considered a real data set. The set consists of various optical images (see Fig. 2). We make both qualitative and quantitative comparisons against the approaches given in [5]. The approaches given in [5] are implemented using the same set of parameters presented in this letter. There are two approaches presented in [5] to analyze the difference image to create the change map: 1) EM-based thresholding and 2) MRF-based thresholding. The former is free of parameter, but the latter depends on the parameter β which tunes the influence of the spatial contextual information on the change detection process. In this letter, we selected $\beta = 1.6$ [5].

In the experiments, $h = 4$ and $S = 3$ are used.[1] Each $h \times h$ block of the difference image could contain one of the three different types of data coming from the difference image: 1) no-change data; 2) change data; and 3) mixture of change and no-change data. The first two cases happen when the $h \times h$ block is completely localized on the changed or unchanged areas of the difference image. The last case happens when the $h \times h$ block is localized on the boundaries between changed and unchanged regions of the difference image. Then, each type of data could be represented with an eigenvector, i.e., $S = 3$. It is worth to note that we perform extensive set of experiments when $3 < S \leq h^2$, and it is observed that there is no significant

[1]The MATLAB implementation of the proposed approach can be asked from celikturgay@gmail.com with the tag [ChangeDetectionPCAkMeans] in the subject line.

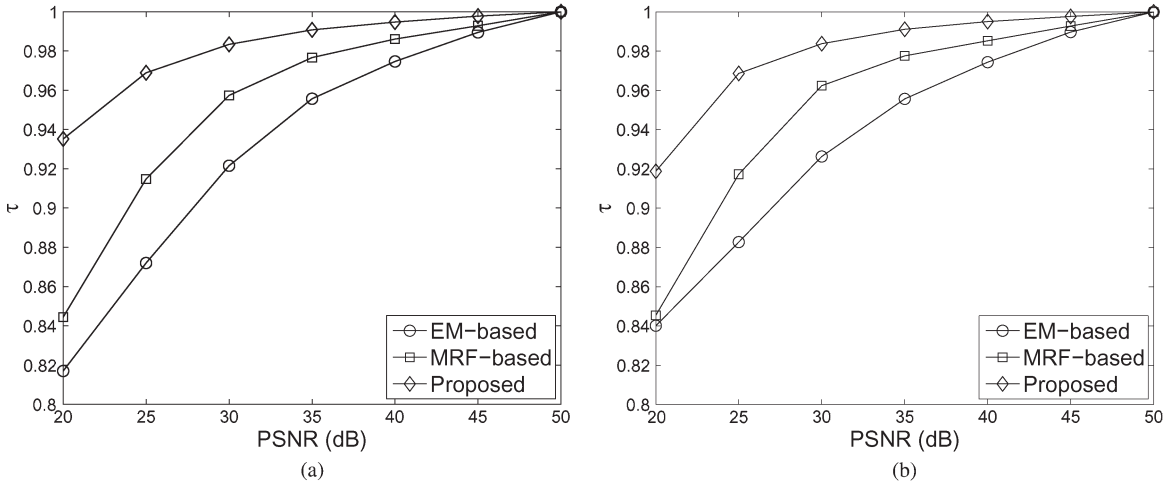

Fig. 3. Detection performance comparisons according to (8) against different levels of noises. (a) Zero-mean Gaussian noise. (b) Speckle noise.

change in the change detection performance with respect to that of $S = 3$.

Fig. 2 shows some qualitative results for the set of optical images. The input images in Fig. 2 are from the various parts of Lake Tahoe, Reno, Nevada, which were captured on August 5, 1986 and August 5, 1992, respectively [9]. Due to drought weather, the input images in the first row show the decrease in the forest canopy [9], and the input images in the second row reveal the changes of the lake's surface area [9]. The input images in the third row show extensive change areas resulted from a forest fire [9]. It is clear, as shown in Fig. 2(c)–(e), that the resultant change maps reflect the changes of the same geographical area taken at two different time instances as aforementioned. It is also clear from qualitative results shown in Fig. 2 that EM-based thresholding [see Fig. 2(c)] holds the highest rate of false detections. The number of false detections is reduced through the use of MRF-based contextual information [see Fig. 2(d)]. Higher values of β provides lower false detections with the expense of higher miss detections. The result of the proposed technique is shown in Fig. 2(e) and provides better qualitative results with respect to the other approaches.

Generally speaking, during the acquisition process of satellite images, different types of noise could be present. Thus, it would be interesting to see how the proposed automatic change detection method is able to combat different types of noise interference. For that, different levels and types of noise are added onto the input image, as shown in the third row in Fig. 2(a). The measure of noise level is defined in terms of peak signal-to-noise ratio (PSNR), in decibels. That is, given an input image $\mathbf{X}$ of size $H \times W$ and its noisy realization $\hat{\mathbf{X}}$, the PSNR measured between the two images is calculated as

$$\text{PSNR} = 10 \log_{10} \left(\frac{HW}{\sum_{i=1}^{H} \sum_{j=1}^{W} \left(x(i,j) - \hat{x}(i,j) \right)^2} \right) \quad (7)$$

where it is assumed that the maximum intensity value of input images is one.

The stability of the change detection algorithm against noise is measured by measuring the difference between two change detection results $\mathbf{CM}_1$ and $\mathbf{CM}_2$, which are created as follows. Given two input images $\mathbf{X}_1$ and $\mathbf{X}_2$, the change detection algorithm is applied to generate $\mathbf{CM}_1$. Then, $\mathbf{X}_1$ is contaminated with noise, and $\mathbf{CM}_2$ is generated to find the change map between noisy $\mathbf{X}_1$ and $\mathbf{X}_2$. The difference between $\mathbf{CM}_1$ and $\mathbf{CM}_2$ is measured as

$$\tau = 1 - \frac{\Sigma_{i=1}^{H} \Sigma_{j=1}^{W} |\text{cm}_1(i,j) - \text{cm}_2(i,j)|}{HW} \quad (8)$$

which reflects the robustness of the change detection algorithm against noise. When $\mathbf{CM}_1$ and $\mathbf{CM}_2$ are the same, τ becomes one, and it approaches to zero when $\mathbf{CM}_2$ differs from $\mathbf{CM}_1$.

The proposed technique uses block-based data analysis to find the subpixel-level resultant change map and is expected to perform better against noise in images with respect to methods proposed by [5]. The MRF-based approach [5] is using 3×3 contextual information to make a final decision on each pixel. This can also be thought as a block-based approach and expected to perform better than the EM-based thresholding. The performance results according to (8) are shown in Fig. 3 for different levels of zero-mean Gaussian noise [see Fig. 3(a)] and speckle noise [see Fig. 3(b)]. It is clear from Fig. 3 that the proposed approach is more stable against different types of noise. The proposed algorithm is fairly robust against the zero-mean Gaussian and speckle noises when PSNR ≥ 20 dB, where the maximum rate of change is 6% for zero-mean Gaussian noise and 8% for speckle noise with respect to no-noise change detection performance. This shows the superiority of the approach.

In the proposed approach, the parameter h defines the local neighborhood so that it affects the contribution of the spatial contextual information on the resultant change map. It is similar to the parameter β in the MRF-based approach [5]. Keeping the value of h large will reduce both the false detections and effects of the noise with the expense of increase in miss detections, and vice versa. This phenomenon is shown in Fig. 4 which shows change detection results on input images shown in the third row of Fig. 2 when different values of h and β are used by the proposed approach and MRF-based approach [5], respectively.

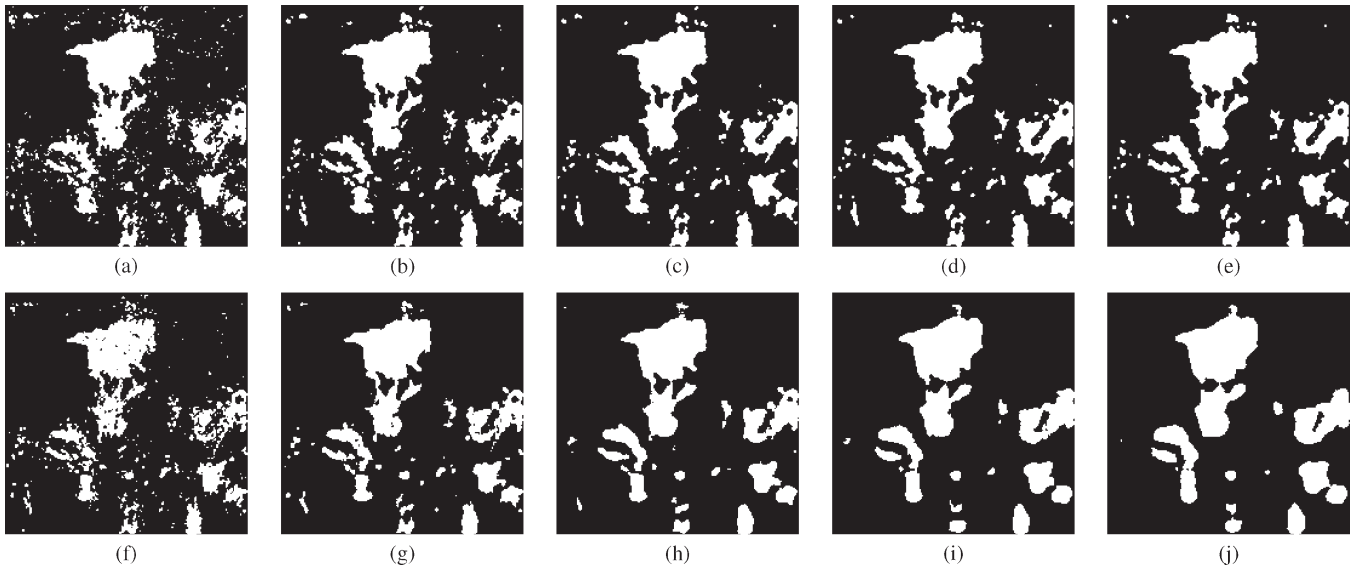

Fig. 4. Change detection results on input images shown in the third row of Fig. 2 when different values of β and h are used for (the first row) MRF-based approach [5] and (the second row) proposed approach, respectively. (a) $\beta = 0.6$. (b) $\beta = 1.6$. (c) $\beta = 2.6$. (d) $\beta = 3.6$. (e) $\beta = 4.6$. (f) $h = 2$. (g) $h = 4$. (h) $h = 6$. (i) $h = 8$. (j) $h = 10$.

IV. Conclusion

An unsupervised change detection technique is developed by conducting k-means clustering on feature vectors which are extracted using $h \times h$ local data projection onto eigenvector space. The eigenvector space is generated using PCA on $h \times h$ nonoverlapping difference image blocks. The proposed method uses $h \times h$ neighborhood to extract feature vector for each pixel so that it automatically considers the contextual information.

The proposed algorithm is simple in computation yet effective in identifying meaningful changes which makes it suitable for real-time applications. It produces results comparable, even better, with the MRF-based approach [5], which requires computationally expensive data modeling and parameter estimation. Simulation results show that the proposed algorithm performs quite well on combating both the zero-mean Gaussian noise and the speckle noise, which is quite attractive for change detection in optical and SAR images.

References

[1] F. Pacifici, F. Del Frate, C. Solimini, and W. Emery, "An innovative neural-net method to detect temporal changes in high-resolution optical satellite imagery," *IEEE Trans. Geosci. Remote Sens.*, vol. 45, no. 9, pp. 2940–2952, Sep. 2007.

[2] F. Bovolo and L. Bruzzone, "A split-based approach to unsupervised change detection in large-size multitemporal images: Application to tsunami-damage assessment," *IEEE Trans. Geosci. Remote Sens.*, vol. 45, no. 6, pp. 1658–1670, Jun. 2007.

[3] S. Ghosh, L. Bruzzone, S. Patra, F. Bovolo, and A. Ghosh, "A context-sensitive technique for unsupervised change detection based on Hopfield-type neural networks," *IEEE Trans. Geosci. Remote Sens.*, vol. 45, no. 3, pp. 778–789, Mar. 2007.

[4] F. Bovolo, L. Bruzzone, and M. Marconcini, "A novel approach to unsupervised change detection based on a semisupervised SVM and a similarity measure," *IEEE Trans. Geosci. Remote Sens.*, vol. 46, no. 7, pp. 2070–2082, Jul. 2008.

[5] L. Bruzzone and D. Prieto, "Automatic analysis of the difference image for unsupervised change detection," *IEEE Trans. Geosci. Remote Sens.*, vol. 38, no. 3, pp. 1171–1182, May 2000.

[6] A. Boucher, K. Seto, and A. Journel, "A novel method for mapping land cover changes: Incorporating time and space with geostatistics," *IEEE Trans. Geosci. Remote Sens.*, vol. 44, no. 11, pp. 3427–3435, Nov. 2006.

[7] P. Gamba, F. Dell'Acqua, and G. Lisini, "Change detection of multitemporal SAR data in urban areas combining feature-based and pixel-based techniques," *IEEE Trans. Geosci. Remote Sens.*, vol. 44, no. 10, pp. 2820–2827, Oct. 2006.

[8] R. C. Gonzalez and R. E. Woods, *Digital Image Processing*, 3rd ed. Upper Saddle River, NJ: Prentice-Hall, 2006.

[9] Southwest U.S. change detection images from the EROS Data Center, (Accessed: March 2009). [Online]. Available: http://geochange.er.usgs.gov/sw/changes/natural/reno-tahoe/